COMMUNICATION

Enhanced efficiency of solution-processed small-molecule solar cells upon incorporation of gold nanospheres and nanorods into organic layers†

Xiaoyan Xu,‡[a] Aung Ko Ko Kyaw,‡[b] Bo Peng,[c] Qingguo Du,[d] Lei Hong,[a] Hilmi Volkan Demir,[ac] Terence K. S. Wong,*[a] Qihua Xiong*[ac] and Xiao Wei Sun*[a]

The significantly enhanced performance upon incorporation of Au nanoparticles in solution-processed small-molecule solar cells is demonstrated. Simultaneously incorporating Au nanospheres into the hole transport layer and Au–silica nanorods into the active layer results in superior broadband absorption improvement in the device with a power conversion efficiency of 8.72% with 31% enhancement.

Solution-processed small molecule (SM) bulk heterojunction (BHJ) organic solar cells are emerging as a competitive alternative to widely studied polymer solar cells (PSC).[1] A power conversion efficiency (PCE) higher than 8% has recently been reported due to the excellent solubility in organic solvents, broadband light absorption and good charge transport property of the solution-processed SM donor.[2] Moreover, this type of SM donor offers simple synthesis, purification and monodispersity compared to polymeric materials.[1d] As with the PSC, SM solar cells are limited by insufficient light absorption because the short exciton diffusion length and low carrier mobilities of organic semiconductor materials necessitate the use of thin active layers.[3] As a result, an approach to enhance light absorption without increasing the thickness of the active layer is necessary. Recently, metallic nanoparticles (NPs) have been widely introduced into PSC for enhanced light harvesting induced by the plasmonic effect of metallic NPs.[4] In the literature, there are reports on plasmonic PSC in which single metallic NPs are incorporated into various layers, for examples: the hole transport layer (HTL),[4b]

active layer[4c] or both.[4d] In addition, two different metallic NPs were blended within a single layer.[4e,f] Despite significant PCE enhancement in PSC, there have been no reports on the plasmonic effect of metallic NPs in solution-processed SM solar cells. In plasmonic devices, the configuration that incorporates metallic NPs into the HTL layer and the active layer results in better hole transport and improved light absorption[4d] while the configuration that combines different shapes of NPs in the active layer achieved a broadband absorption enhancement.[4e] However, embedding NPs with two different shapes into the HTL layer and the active layer, respectively, in order to leverage advantages of both configurations, has not been reported yet.

In this communication, we report high-performance solution-processed SM solar cells by incorporation of Au nanospheres into the poly(3,4-ethylene-dioxythiophene):poly(styrenesulphonate) (PEDOT:PSS) layer and Au–silica nanorods into the 7,7′-(4,4-bis(2-ethylhexyl)-4H-silolo[3,2-b:4,5-b']-dithiophene-2,6-diyl)bis(6-fluoro-4-(5′-hexyl-[2,2′-bithiophen]-5-yl)benzo[c][1,2,5]thiadiazole):[6,6]-phenyl-C_{71}-butyric acid methyl ester (p-DTS(FBTTh$_2$)$_2$:PC$_{70}$BM) layer, simultaneously. Thus far, only a few reports have described the metallic nanorods with larger size which have a longer extinction wavelength and a wide absorption spectrum enhancement up to 700 nm. These nanorods can give rise to both plasmonic and scattering effects.[5] A combination of Au nanospheres and Au–silica nanorods in organic layers provides a broader optical absorption enhancement and better hole transport. As a result, significantly improved PCE is realized by incorporating dual Au NPs.

Fig. 1a–d shows molecular structures of p-DTS(FBTTh$_2$)$_2$ and PC$_{70}$BM, SM device structure, and the transmission electron microscopy (TEM) images of Au nanospheres and Au–silica nanorods, respectively. Au NPs were synthesized using the seed-mediated method.[5b,c] Au nanospheres have an average diameter of about 10 nm. Au–silica nanorods are completely and uniformly coated by 6 nm silica shells and have an average length and diameter of 89 nm and 34 nm respectively. The normalized UV-vis absorption spectra of Au nanospheres in water and Au–silica nanorods in chlorobenzene (CB) were measured. Fig. 1e shows that the maximum absorption peaks of Au nanospheres and Au–silica

[a] NOVITAS, Nanoelectronics Centre of Excellence, School of Electrical and Electronic Engineering, Nanyang Technological University, Singapore 639798, Singapore. E-mail: ekswong@ntu.edu.sg, qihua@ntu.edu.sg, EXWSun@ntu.edu.sg

[b] Institute of Materials Research and Engineering (IMRE), Agency for Science Technology and Research (A*STAR), Singapore 117602, Republic of Singapore

[c] School of Physical and Mathematical Sciences, Nanyang Technological University, Singapore 639798, Singapore

[d] Institute of High Performance Computing, 1 Fusionopolis Way, #16-16 Connexis North, Singapore 138632, Republic of Singapore
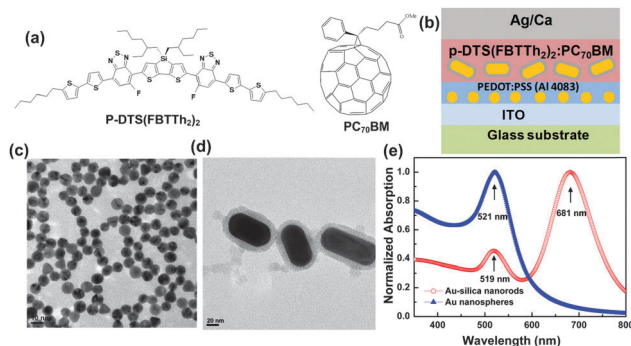
Fig. 1 (a) Molecular structures of *p*-DTS(FBTTh₂)₂ and PC₇₀BM, (b) device structure of the SM solar cell, (c) TEM image of Au nanospheres, (d) TEM image of Au–silica nanorods and (e) normalized UV-Vis absorption spectra of Au nanospheres in water and Au–silica nanorods in CB.

Table 1 Photovoltaic parameters of SM BHJ devices with Au NPs in different layers under AM 1.5G illumination at 100 mW cm⁻²

Device	J_{SC} (mA cm^{-2})	V_{OC} (V)	FF (%)	PCE (%)
A	12.17 ± 0.32	0.77 ± 0.01	69.65 ± 0.65	6.52 ± 0.15
B	13.53 ± 0.36	0.77 ± 0.01	71.20 ± 0.79	7.41 ± 0.22
C	14.96 ± 0.30	0.77 ± 0.01	70.58 ± 0.44	8.11 ± 0.17
D	15.56 ± 0.37	0.77 ± 0.01	71.51 ± 0.75	8.54 ± 0.22

nanorods were at 521 and 681 nm, respectively. Here, four types of SM solar cells were fabricated (Device A: reference device without NPs; B: Au nanospheres in PEDOT:PSS only; C: Au–silica nanorods in the active layer only; D: NPs in both PEDOT:PSS and the active layers). The atomic force microscopy (AFM) images of the PEDOT:PSS layer and the active layer in Fig. S1 (ESI†) show that the root-mean-square (RMS) roughness of PEDOT:PSS films increases from 0.872 nm to 0.899 nm and that of the *p*-DTS(FBTTh₂)₂:PC₇₀BM films increases from 1.677 nm to 1.840 nm upon incorporating NPs. The almost unchanged RMS roughness confirms that all the NPs are embedded within the PEDOT:PSS layer and the active layer and would not affect their morphologies.

The current density–voltage (*J–V*) characteristics of the four devices with Au NPs incorporated into different layers are shown in Fig. 2a. The average photovoltaic parameters from ten identical devices for each type are listed in Table 1. The effect of Au NP concentration incorporated into single organic layers of SM solar cells was also studied and the corresponding *J–V* curves are shown in Fig. S2 (ESI†). Then, we studied the effect of Au NPs incorporated in both HTL and the active

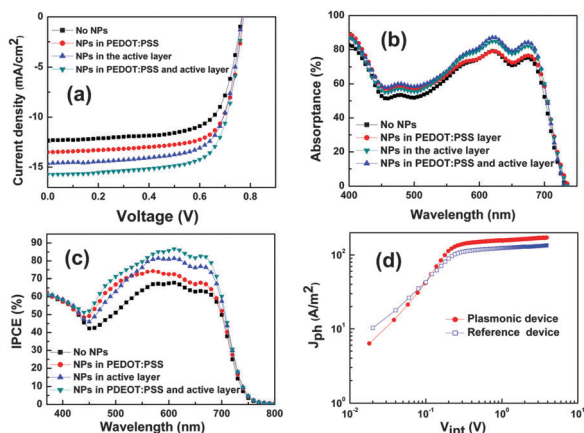layer simultaneously. The reference device has an average PCE of 6.52 ± 0.15% with an open-circuit voltage (V_{OC}) of 0.77 ± 0.01 V, a short-circuit current density (J_{SC}) of 12.17 ± 0.32 mA cm⁻² and a fill factor (FF) of 69.65 ± 0.65%. After incorporation of Au nanospheres only in the PEDOT:PSS layer, the V_{OC} of the plasmonic device remained the same, J_{SC} and FF both increased to 13.53 ± 0.36 mA cm⁻² and 71.2 ± 0.79%, respectively, leading to an average PCE of 7.41 ± 0.22%. Besides, the series resistance (R_S) of the plasmonic device, extracted from the dark *J–V* curve, reduced from 2.75 to 2.04 Ω cm² which contributes to an increase of FF. When only Au–silica nanorods are incorporated into the active layer, V_{OC} and R_S remained the same and FF increased slightly to 70.58 ± 0.44%. In contrast, J_{SC} has a larger enhancement to 14.96 ± 0.30 mA cm⁻² than the previous plasmonic device, which is due to the broader absorption spectrum of Au–silica nanorods that extends to longer wavelengths relative to Au nanospheres. Upon doping Au NPs into both the PEDOT:PSS layer and the active layer, J_{SC} and FF further improved to 15.56 ± 0.37 mA cm⁻² and 71.51 ± 0.75% while the V_{OC} remained unchanged, resulting in a much better PCE of 8.54 ± 0.22% (with a maximum value of 8.72%).

To verify that the improved J_{SC} is due to the optical effect of Au NPs, we performed the UV-vis absorption and the incident photon to current conversion efficiency (IPCE) measurements. Fig. 2b and c shows that the absorption and IPCE spectra of the active layer are both enhanced in the spectral region of 420 to 550 nm after incorporation of Au nanospheres only into the PEDOT:PSS layer, and further improvement in the spectral range of 460 to 720 nm is evident after incorporation of Au–silica nanorods only into the active layer. In addition, broader light absorption and IPCE spectra covering from 420 to 720 nm are obtained upon combining dual Au NPs in the devices. Such enhanced absorption and IPCE spectra are well matched with the plasmonic resonance region of Au nanospheres and Au–silica nanorods.

To further confirm the effect of Au NPs on the optical absorption of the SM solar cell, we determined the maximum photoinduced carrier generation rate (G_{max}) in devices with and without dual NPs.[6] Fig. 2d reveals the dependence of the photocurrent density (J_{ph}) on the internal voltage (V_{int}) for reference and plasmonic devices. J_{ph} is determined as $J_{ph} = J_L - J_D$, where J_L and J_D are the current density under illumination and in the dark, respectively. V_{int} is calculated as $V_{int} = V_0 - V_a$, where V_0 is the voltage at which $J_{ph} = 0$ and V_a is the applied voltage.[6a] Fig. 2d shows that J_{ph} increases linearly at a low V_{int} and saturates at a high V_{int} (2 V and above), which is large enough to dissociate all the photogenerated excitons into free

Fig. 2 (a) *J–V* characteristics of solar cells with and without the optimized concentration of NPs, (b) UV-Vis absorption spectra of *p*-DTS(FBTTh₂)₂:PC₇₀BM BHJ films with and without NPs, (c) IPCE spectra of solar cells with and without NPs and (d) photocurrent density (J_{ph}) *versus* internal voltage (V_{int}) characteristics of the reference device and the dual NP device.
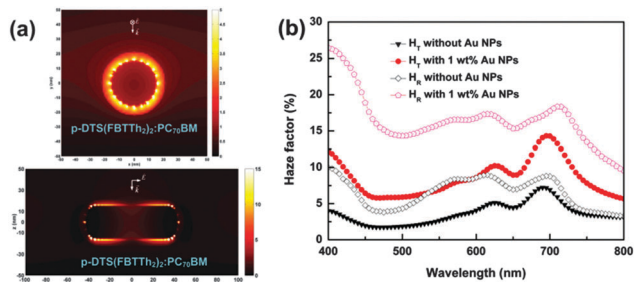
Fig. 3 (a) Electric field intensity distribution around Au–silica nanorods at 680 nm in side view and front view and (b) transmission and reflection haze factor spectra of the p-DTS(FBTTh$_2$)$_2$:PC$_{70}$BM film with and without 1 wt% of Au nanorods.
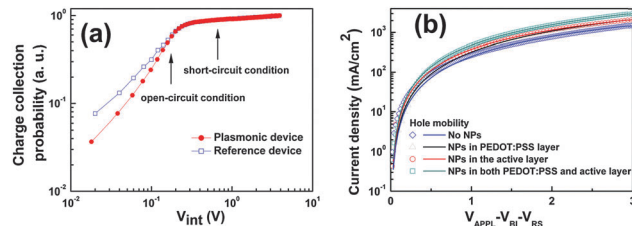

Fig. 4 (a) Charge collection probability (P_C) versus internal voltage (V_{int}) characteristics of the reference device and the dual NP device and (b) the dark J–V characteristics of hole-only devices with and without Au NPs.

charge carriers and collect them at the electrodes. Thus, at a high V_{int}, the saturation current density (J_{sat}) is only limited by the total number of absorbed photons. G_{max} could be calculated from $J_{sat} = qLG_{max}$, where q is the electronic charge and L is the thickness of the active layer.[6b] The value of G_{max} for the reference device and the plasmonic device is 8.43×10^{27} m^{-3} s^{-1} ($J_{sat} = 135$ A m^{-2}) and 1.07×10^{28} m^{-3} s^{-1} ($J_{sat} = 172$ A m^{-2}), respectively. A significant enhancement of G_{max} occurred after incorporating dual Au NPs. Since G_{max} corresponds to the maximum number of absorbed photons, such enhancement demonstrates increased light absorption in the device with dual NPs.

The mechanisms of enhanced light absorption by Au NPs are studied by the finite-difference time-domain (FDTD) method and diffuse scattering measurements.[7] Fig. 3a shows the distribution of field intensity around the Au–silica nanorods at 680 nm. It is found that the field intensity is increased by a factor of 2 relative to the incident light outside the silica shell which will increase absorption within the active layer. Moreover, the haze factor spectra for transmission (H_T) and reflection (H_R) are measured by dividing the diffuse transmission/reflection by the total transmission/reflection. Fig. 3b shows the increase in both H_T and H_R upon incorporating the Au–silica nanorods, suggesting that NPs scatter more light to increase the optical path. Therefore, both plasmonic and scattering effects excited by NPs contribute to light absorption in SM solar cells.

Fig. 4a shows the charge collection probability (P_C) versus V_{int}. The P_C could be obtained by normalizing J_{ph} by J_{sat}.[6c] The P_C under short-circuit conditions ($V_a = 0$ V) increases from 88.1% to 91.3% upon addition of dual Au NPs, indicating that the incorporation of Au NPs has a positive influence on the charge collection by electrodes. The value of P_C is higher than in PSCs and it decreased slowly from short-circuit conditions to open-circuit conditions compared to the sharp increase in some polymers.[8] This indicates that there is less recombination which thus results in high photocurrent and fill factor in the p-DTS(FBTTh$_2$)$_2$:PC$_{70}$BM device.

Since carrier mobility is an important factor for charge transport and mainly limited by the hole transport in our devices,[6a] holy-only devices were fabricated to determine the hole mobility. The dark J–V characteristics of hole-only devices

are measured and fitted using the space-charge limited current (SCLC) model and the Mott–Gurney law that includes field-dependent mobility,[9] as shown in Fig. 4b. Upon incorporation of Au NPs into the PEODT:PSS layer only, the active layer only and both layers, the zero field hole mobility slightly increased from 1.26×10^{-3} cm^2 V^{-1} s^{-1} to 1.41×10^{-3} cm^2 V^{-1} s^{-1}, 2.07×10^{-3} cm^2 V^{-1} s^{-1} and 2.28×10^{-3} cm^2 V^{-1} s^{-1} respectively. An increase in the hole moblities indicates that the incorporation of the Au NPs does not adversely affect the charge transport in the active layer.

In conclusion, we demonstrate the maximum PCE of 8.72% with a relative performance increase of 31% in solution-processed SM solar cells by incorporation of Au nanospheres and Au–silica nanorods into organic layers. Absorption spectra, IPCE spectra and G_{max} confirm that the combination of Au NPs with two different shapes realized a broadband absorption improvement in the SM solar cells. The studied mechanisms of enhanced light absorption ascribe to both plasmonic and scattering effects by Au NPs. Enhanced carrier collection and carrier transport properties ensure the good performance in plasmonic devices. Therefore, apart from contributing to light absorption within the active layer, the Au nanospheres in the PEDOT:PSS layer can facilitate the hole collection and Au–silica nanorods in the active layer avoid the carrier recombination at the metal surface by insulating silica shells.

Notes and references

1 (a) W. Cambarau, A. Viterisi, J. W. Ryan and E. Palomares, Chem. Commun., 2014, DOI: 10.1039/c3cc47333c; (b) T. S. van der Poll, J. A. Love, T.-Q. Nguyen and G. C. Bazan, Adv. Mater., 2012, 24, 3646–3649; (c) Y. Sun, G. C. Welch, W. L. Leong, C. J. Takacs, G. C. Bazan and A. J. Heeger, Nat. Mater., 2012, 11, 44–48; (d) Y. Lin, Y. Li and X. Zhan, Chem. Soc. Rev., 2012, 41, 4245–4272; (e) Y. Yang, J. Zhang, Y. Zhou, G. Zhao, C. He, Y. Li, M. Andersson, O. Inganäs and F. Zhang, J. Phys. Chem. C, 2010, 114, 3701–3706.
2 (a) A. K. K. Kyaw, D. H. Wang, D. Wynands, J. Zhang, T.-Q. Nguyen, G. C. Bazan and A. J. Heeger, Nano Lett., 2013, 13, 3796–3801; (b) A. K. K. Kyaw, D. H. Wang, V. Gupta, W. L. Leong, L. Ke, G. C. Bazan and A. J. Heeger, ACS Nano, 2013, 7, 4569–4577.
3 S. R. Forrest, MRS Bull., 2005, 30, 28–32.
4 (a) E. Stratakis and E. Kymakis, Mater. Today, 2013, 16, 133–146; (b) J.-L. Wu, F.-C. Chen, Y.-S. Hsiao, F.-C. Chien, P. Chen, C.-H. Kuo, M. H. Huang and C.-S. Hsu, ACS Nano, 2011, 5, 959–967; (c) D. H. Wang, D. Y. Kim, K. W. Choi, J. H. Seo, S. H. Im, J. H. Park, O. O. Park and A. J. Heeger, Angew. Chem., Int. Ed., 2011, 50, 5519–5523; (d) F. X. Xie,

W. C. H. Choy, C. C. D. Wang, W. E. I. Sha and D. D. S. Fung, *Appl. Phys. Lett.*, 2011, **99**, 153304; (*e*) X. Li, W. C. H. Choy, H. Lu, W. E. I. Sha and A. H. P. Ho, *Adv. Funct. Mater.*, 2013, **23**, 2728–2735; (*f*) L. Lu, Z. Luo, T. Xu and L. Yu, *Nano Lett.*, 2012, **13**, 59–64.

5 (*a*) K. S. Lee and M. A. El-Sayed, *J. Phys. Chem. B*, 2005, **109**, 20331–20338; (*b*) X. Xu, A. K. K. Kyaw, B. Peng, D. Zhao, T. K. S. Wong, Q. Xiong, X. W. Sun and A. J. Heeger, *Org. Electron.*, 2013, **14**, 2360–2368; (*c*) T. Ming, L. Zhao, Z. Yang, H. Chen, L. Sun, J. Wang and C. Yan, *Nano Lett.*, 2009, **9**, 3896–3903.

6 (*a*) S. R. Cowan, A. Roy and A. J. Heeger, *Phys. Rev. B*, 2010, **82**, 245207; (*b*) V. D. Mihailetchi, L. J. A. Koster, J. C. Hummelen and

P. W. M. Blom, *Phys. Rev. Lett.*, 2004, **93**, 216601; (*c*) V. D. Mihailetchi, H. X. Xie, B. de Boer, L. J. A. Koster and P. W. M. Blom, *Adv. Funct. Mater.*, 2006, **16**, 699–708.

7 (*a*) N. Lagos, M. M. Sigalas and E. Lidorikis, *Appl. Phys. Lett.*, 2011, **99**, 063304; (*b*) Y.-S. Hsiao, C.-P. Chen, C.-H. Chao and W.-T. Whang, *Org. Electron.*, 2009, **10**, 551–561.

8 M. Lenes, M. Morana, C. J. Brabec and P. W. M. Blom, *Adv. Funct. Mater.*, 2009, **19**, 1106–1111.

9 (*a*) C. Melzer, E. Koop, V. Mihailetchi and P. Blom, *Adv. Funct. Mater.*, 2004, **14**, 865–870; (*b*) P. N. Murgatroyd, *J. Phys. D: Appl. Phys.*, 1970, **3**, 151.